ANL/NE-15/39

A SCOPING ANALYSIS OF THE IMPACT OF SiC CLADDING ON LATE-PHASE ACCIDENT PROGRESSION INVOLVING CORE–CONCRETE INTERACTION

About Argonne National Laboratory
Argonne is a U.S. Department of Energy laboratory managed by UChicago Argonne, LLC under contract DE-AC02-06CH11357. The Laboratory's main facility is outside Chicago, at 9700 South Cass Avenue, Argonne, Illinois 60439. For information about Argonne and its pioneering science and technology programs, see www.anl.gov.

DOCUMENT AVAILABILITY

Online Access: U.S. Department of Energy (DOE) reports produced after 1991 and a growing number of pre-1991 documents are available free via DOE's SciTech Connect (http://www.osti.gov/scitech/)

Reports not in digital format may be purchased by the public from the National Technical Information Service (NTIS):
U.S. Department of Commerce
National Technical Information Service
5301 Shawnee Rd
Alexandria, VA 22312
www.ntis.gov
Phone: (800) 553-NTIS (6847) or (703) 605-6000
Fax: (703) 605-6900
Email: **orders@ntis.gov**

Reports not in digital format are available to DOE and DOE contractors from the Office of Scientific and Technical Information (OSTI):
U.S. Department of Energy
Office of Scientific and Technical Information
P.O. Box 62
Oak Ridge, TN 37831-0062
www.osti.gov
Phone: (865) 576-8401
Fax: (865) 576-5728
Email: **reports@osti.gov**

Disclaimer
This report was prepared as an account of work sponsored by an agency of the United States Government. Neither the United States Government nor any agency thereof, nor UChicago Argonne, LLC, nor any of their employees or officers, makes any warranty, express or implied, or assumes any legal liability or responsibility for the accuracy, completeness, or usefulness of any information, apparatus, product, or process disclosed, or represents that its use would not infringe privately owned rights. Reference herein to any specific commercial product, process, or service by trade name, trademark, manufacturer, or otherwise, does not necessarily constitute or imply its endorsement, recommendation, or favoring by the United States Government or any agency thereof. The views and opinions of document authors expressed herein do not necessarily state or reflect those of the United States Government or any agency thereof, Argonne National Laboratory, or UChicago Argonne, LLC.

ANL/NE-15/39

A SCOPING ANALYSIS OF THE IMPACT OF SiC CLADDING ON LATE-PHASE ACCIDENT PROGRESSION INVOLVING CORE–CONCRETE INTERACTION

M. T. Farmer

Nuclear Engineering
Argonne National Laboratory

November 2014

1. INTRODUCTION

By definition, evaluations of accident tolerant fuel (ATF) must include performance under severe accident conditions. Although various initiators can be postulated, the course of a severe accident for a light water reactor (LWR) usually includes loss of core cooling, core uncovery, heatup, fuel and cladding degradation and failure, and fission product release. During the course of the accident progression, kinetically controlled phenomena alter the physical and chemical states of the core constituents, resulting in a continuous evolution of thermodynamic equilibria.

Experimental studies related to the performance of some constituents of proposed ATF concepts in steam environments at high temperature and pressure have recently been performed [1,2]. These studies have quantified important kinetic phenomena for ATF constituents, such as oxidation rates. Using this information as input, preliminary assessments of ATF performance under severe accident conditions have been carried out with system-level codes [3-5]. In a related study focused on late phase severe accident behavior, some simple metrics for evaluating ATF performance were developed, including ex-vessel molten core–concrete interaction (MCCI) [6]. In this work, essentially all the kinetic limitations on the time-dependent transformation of the core constituents were omitted, and simple thermodynamic boundary conditions for such scenarios were applied. Although conservative in nature, this exercise provided a useful perspective when various ATF concepts are under consideration to replace the UO_2–Zr alloy fuel system in LWRs. A conceptual timeline that illustrates potential oxidation pathways for ATFs during a severe accident is shown in Figure 1. The fit of this ranking method into the overall accident sequence with respect to time interval is also indicated in the figure.

With this background, the overall objective of the current work is to carry out a scoping analysis to determine the impact of ATF on late phase accident progression; in particular, the molten-core concrete interaction portion of the sequence that occurs after the core debris fails the reactor vessel and relocates into containment. This additional study augments previous work [6] by including kinetic effects that govern chemical reaction rates during core-concrete interaction. The specific ATF considered as part of this study is SiC-clad UO_2.

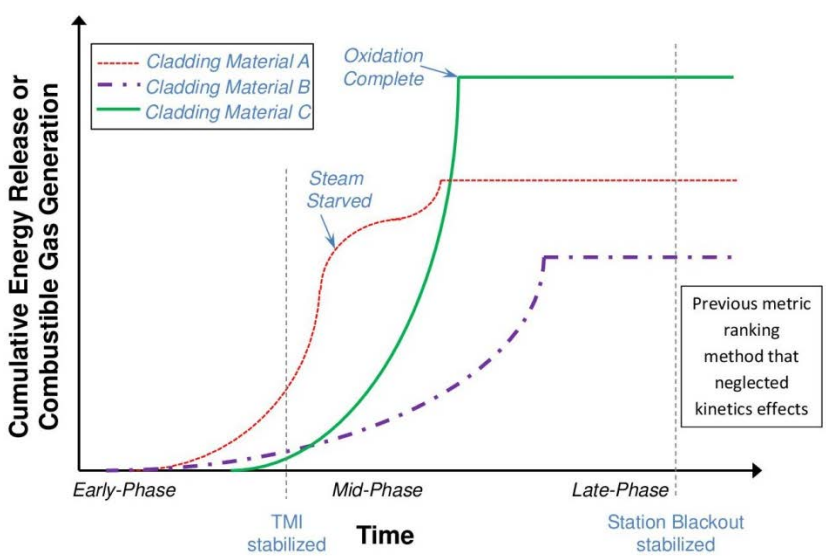

Figure 1. Conceptual illustration of potential oxidation pathways for ATFs during a severe accident [6].

2. CODE UPGRADE METHODOLOGY

The approach taken to carry out this work was to make appropriate upgrades to the CORQUENCH code [7] that calculates MCCI behavior under both wet and dry cavity conditions to account for the different melt constituents and chemical reactions expected for a SiC clad UO_2 system. This code was used as part of DOE-NE's post-Fukushima analysis activities [8]. Under ex-vessel MCCI conditions, oxidizing gases arising from concrete decomposition include H_2O (from free water and hydroxides) and CO_2 (from carbonates). Metals arising from cladding and structural steel degradation in a conventional Zircaloy clad reactor system include Zr, Cr, Fe, and Ni; these elements are listed in Table 1 in their expected order of oxidation based on the stability of their corresponding oxides as they appear in an Ellingham diagram [9]. This table also shows the expected oxidation reactions for each metal for both H_2O and CO_2 concrete decomposition gases. The amounts of Fe_2O_3, Fe_3O_4, and NiO generated in oxidation reactions (at least for ex-vessel conditions) are small, so the corresponding reactions are ignored in this work. Depending upon core temperature and pressure during degradation, the additional melt constituents expected based on thermodynamic equilibria calculations for the SiC-clad UO_2 fuel system include Si metal and SiC [6]. As is evident from Table 1, Si metal would be preferentially oxidized before the structural steel metals, which is consistent with Zr. The oxidation energy for Si is also noted to be relatively high.

In terms of upgrades that were made to CORQUENCH in order to treat SiC-clad fuel, the first step was to restructure the code to include Si and SiC as melt constituents. The metals oxidation hierarchy was also restructured to include Si according to the scheme outlined in Table 1. Silicon metal that is oxidized is mapped into SiO_2 (already treated since it is a principal constituent of most concretes) based on the code conservation of mass equations. The reaction rate of the Si metal was assumed to be controlled by the rate of concrete decomposition gas production during core-concrete interaction (test data indicates that this is a valid assumption [10]). At this point, the thermochemistry of LWR core debris containing residual refractory SiC has not been fully explored. As noted earlier, limited thermodynamic equilibrium calculations [6] indicate that for a given temperature and pressure, some amount SiC would remain in the core debris in equilibrium with the other chemical species. Thus, for the purposes of this work any SiC present in the debris relocated from the reactor vessel was assumed to reside in the oxide phase (consisting of UO_2, concrete, and structural steel oxides). Furthermore, this material was treated as chemically inert, and was assumed to sublimate at its own unique melting temperature within the oxide phase. Finally, it was further assumed that the phase diagram data for the balance of remaining oxides are not affected by the presence of this refractory carbide. This assumption was required to move forward with this analysis given the current limitations on thermochemical modeling within CORQUENCH, but it needs to be explored through experiments and additional thermodynamic analyses.

Table 1. Metal oxidation reactions (reactions heat evaluated at 2100 °C) [6].

Oxidation Sequence	Metal	Oxidation Reactions
1	Zr	$Zr + 2H_2O \rightarrow ZrO_2 + 2H_2 + 6.6\ MJ/kg_{Zr}$ $Zr + 2CO_2 \rightarrow ZrO_2 + 2CO + 6.1\ MJ/kg_{Zr}$
2	Si	$Si + 2H_2O \rightarrow SiO_2 + 2H_2 + 15\ MJ/kg_{Si}$ $Si + 2CO_2 \rightarrow SiO_2 + 2CO + 14\ MJ/kg_{Si}$
3	Cr	$2Cr + 3H_2O \rightarrow Cr_2O_3 + 3H_2 + 2.8\ MJ/kg_{Cr}$ $2Cr + 3CO_2 \rightarrow Cr_2O_3 + 3CO + 2.1\ MJ/kg_{Cr}$
4	Fe	$Fe + H_2O \rightarrow FeO + H_2 + 0.04\ MJ/kg_{Fe}$ $Fe + CO_2 + 0.4\ MJ/kg_{Fe} \rightarrow FeO + CO$

Revisions to the property subroutines were made to account for the presence of Si and SiC in the corium enthalpy-temperature, thermal conductivity, density, melt solid fraction, and crust mechanical strength evaluations. Thermophysical property data used for these modifications are summarized in Table 2, while the mechanical property data are provided in Table 3 along with the data for the other corium constituents treated in CORQUENCH. This latter information will be referred to later in the report. Other properties calculated by the code include emissivity and melt viscosity. Silicon metal was lumped into the metal phase constituents treated by the code, and the existing subroutines were then used to evaluate metal phase emissivity and viscosity treating Si as steel. As noted earlier, SiC was assumed to reside in the oxide phase. In terms of emissivity, SiC was assigned the same value as the other oxides (i.e. 0.83). In terms of viscosity, the presence of SiC was assumed to have no impact on the liquid component of the oxide-phase viscosity. However, the presence of solid SiC was incorporated into the overall solid fraction evaluation for the oxide phase. The augmentation in viscosity due to the presence of the solid was then calculated using the methodology already implemented in the code [7].

Table 2. Thermophysical Property Data Assumed for Si and SiC.

Material Property	Si	SiC	Note(s)
Melting Point (K)	1687 [12]	3003 [11]	
Solid phase specific heat (J/kg-K)	933 [12]	1227 [13]	
Heat of Fusion (kJ/kg)	1790 [12]	1625 [14]	
Liquid phase specific heat (J/kg-K)	971 [12]	1575 [14]	
Solid phase conductivity (W/m-K)	See note	26.3	For Si, curve fit to data in [15] from 300 K to the melting point; for solid SiC, data from [11] at 1770 K.

Liquid phase thermal conductivity (W//m-K)	65 [15]	N/A	SiC sublimates near the melting point
Solid phase density (kg/m^3)	2330	3080 [11]	
Liquid phase density (kg/m^3)	2570	N/A	SiC sublimates near the melting point

Table 3. Crust Constituent Mechanical Properties Assumed in CORQUENCH [7]. (The additional properties implemented for SiC-clad ATF analysis are shown in blue)

Corium Constituent	Elastic Modulus (GPa)	Tensile Strength (MPa)	Linear Expansion Coefficient (10^{-6} m/m-K)
UO_2	190	117	9.5
ZrO_2	250	80	7.5
Cr_2O_3	200	70	5.4
Fe_2O_3	306	100	12.5
SiO_2	72	50	0.9
CaO	175	77	12.6
MgO	308	129	11.6
Al_2O_3	470	270	7.0
Zircaloy-2	95	300	6.5
Stainless Steel	193	340	17.2
Si	170 [15]	300[16]	2.5[17]
SiC	380	250	5.0

3. SCENARIO DEFINITIONS

3.1 Melt Pour Conditions

In terms of applications to plant accident scenarios, the melt pour conditions from the RPV predicted by system levels codes such as MAAP and MELCOR [8] are input into CORQUENCH for analysis of MCCI behavior. A scenario leading to this type of behavior is an unmitigated Station Blackout (SBO) such as that which occurred at Fukushima Unit 1 (1F1). As noted in Section 1, analyses of these scenarios with system level codes upgraded for ATFs are limited in the literature [3-5]. A recent study was conducted by Robb [4] in which an upgraded version of MELCOR was applied to a BWR SBO utilized FeCrAl-clad UO_2 fuel. The results of this study indicated that the use of this advanced cladding delayed but did not prevent eventual failure of the RPV and discharge of core melt into containment. Unfortunately, CORQUENCH is not able to treat this particular ATF-type at the current time due to the fact that Al is not treated as

a melt constituent. Thus, the melt pour conditions predicted in this study cannot be used for further analysis here.

On this basis, some simplifying assumptions were made in order to derive a hypothetical, late phase core melt composition that one might expect for a SiC clad – UO_2 fuel system for an extended SBO sequence. This approach relies on findings from the earlier study examining potential fuel degradation behavior for ATFs [6]. Since extensive analyses with MAAP and MELCOR were carried for Fukushima Unit 1 (1F1) as part of DOE and industry-supported studies [8,19,20], this scenario was selected for further analysis here. Table 4 provides the melt pour conditions based on these simulations for Unit 1, which was a Mark I BWR with conventional Zircaloy-clad UO_2 fuel.

In order to estimate what an ex-vessel core-melt composition might look like for a similar Mark I scenario involving SiC fuel, the following assumptions were made. First, the equivalent cladding volume in the core melt was assumed to be replaced by an equal volume of SiC, which effectively assumes that in-core Zircaloy present as cladding and channel boxes is replaced by SiC of equal thickness. Second, the speciation of Si and SiC in the ex-vessel melt was assumed to be the same as that determined on the basis of thermodynamic equilibrium calculations [6] given the melt pour temperatures estimated by the two codes (i.e., 2750 K for the MAAP simulation versus 1850-2100 K for the MELCOR simulation. As a side note, the large difference in melt pour conditions is currently being investigated as part of a cross-walk activity between the two code development teams [21]). Third, given the extent of in-vessel cladding oxidation by steam predicted by the two codes (in terms of a percentage), the equivalent fraction of free Si metal within the melt was assumed to be oxidized to SiO_2. Fourth, the extent of structural steel melting is assumed to be the same regardless of cladding type. The underlying reasoning behind this set of assumptions is that unless the core is cooled, eventually the core melt will evolve to contain a fuel-clad mixture indicative of the in-core composition, the SiC will decompose as the system evolves towards thermodynamic equilibrium, and the extent of oxidation of any free metals in the melt will be controlled by the thermal-hydraulic assumptions built into each system level code that govern the extent of steam-fuel-clad contact. This perception remains to be verified through additional analysis and experiments.

With this background, the corresponding initial ex-vessel core melt composition estimated for the MAAP and MELCOR sequences are shown in Table 4. Due to the high initial melt temperature for the MAAP case, there is a significant amount of Si present in the melt. In contrast, due to the low MELCOR temperature, most of the clad remains as SiC. In terms of ramifications on melt pour conditions, given the changes made to the code, for the MAAP scenario the oxide and metal phase solidus and liquidus temperatures are impacted somewhat by the change in composition, but the initial thermalhydraulic conditions are not; i.e., a highly fluid core melt remains as the predicted initial condition. The fact that the basic physical characteristics of the core melt are not radically affected when the conventional fuel-clad system is replaced with ATF for the MAAP SBO simulation lends a minor amount of credibility to the heuristic arguments used to derive that composition.

Table 4. 1F1 Core Melt Compositions at Vessel Failure Based on MAAP and MELCOR Analyses, Along with Estimated Compositions for an Equivalent Sequence with ATF.

Melt Constituent	MAAP Low Pressure Scenario (kg)		MELCOR Scenario (kg)	
	Zr Clad [20]	SiC Clad estimate	Zr Clad [19]	SiC Clad estimate
SiO_2	0	6023	0	211
FeO	11211	11211	230	230
Fe	16095	16095	20430	20430
Cr	1136	1136	5900	5900
NiO	556	556	2530	2530
Zr	16594	0	25800	0
ZrO_2	14142	0	16600	0
B_4C	502	502	0	0
Si	0	4452	0	207
SiC	0	3152	0	18602
Cr_2O_3	2732	2732	30	30
NiO	1208	1208	30	30
UO_2	76153	76153	69400	69400
Total	140329	123220	140950	117570
Mixture density (g/cc)	7.195	6.188	7.305	6.392
Mass to fill sump (kg)	36332	31248	36890	32280

However, for the MELCOR simulation, the ATF substitution radically affects CORQUENCH predictions of the oxide phase solidus-liquidus temperatures that results in an unrealistic relationship between the melt temperature predicted by MELCOR for the conventional fuel-clad system (i.e. 1950-2100 K) in comparison to what would be required to liquefy the oxide so that it could relocate ex-vessel for the ATF composition. The reason behind this is as follows. Sub-stoichiometric core oxide mixtures [i.e., $(U,Zr)O_{2-x}$] similar to those predicted by MAAP and MELCOR for the conventional fuel-clad system (Table 4) are known to have much lower solidus-liquidus temperatures relative to fully oxidized [$(U,Zr)O_2$] core melt mixtures [22]. Thus, when the metallic Zr in the MELCOR composition is replaced by SiC using the heuristic approach proposed here, the oxide phase freezing temperature range is predicted to increase by hundreds of degrees relative to the conventionally clad system, resulting in a situation in which the core melt would essentially be solid at the core debris temperatures predicted by MELCOR. In order to obtain a molten state, the MELCOR melt temperature would need to be artificially increased, but this increase in temperature would then change the speciation of Si and SiC in the melt that one would predict based on thermodynamic equilibrium calculations [6] from that shown in Table 4. Due to these inconsistencies involved with the current approach for deriving a potential ATF melt composition for the MELCOR scenario, the MCCI calculations with CORQUENCH presented in the next section focus solely on MAAP melt pour conditions.

3.2 Other Input Modeling Assumptions

Aside from assumptions regarding melt composition and temperature, CORQUENCH requires other input data to be specified in order to carry out the simulation. Assumptions regarding these data are provided below.

In the Fukushima Unit 1 calculations carried out previously as part of the DOE-sponsored analyses with MELTSPREAD and CORQUENCH [8], a spatially dependent MCCI analysis was applied within the 1F1 containment. This level of detail is beyond the current scope of work. Rather, an isolated analysis of MCCI behavior within the sumps is performed as this represents the worst-case scenario with respect to evaluating the maximum extent of concrete ablation. Internal to the pedestal, there are two rectilinear drywell sumps, each 1.45 m by 1.45 m in cross-section and 1.2 m deep. These two sumps were combined into a single geometric entity that consists of a cylinder that is 2.23 m in diameter and 1.2 m deep. Thus the sump volume, cross-sectional areas, and depth are conserved as part of this analysis. The sumps were assumed to be completely filled with core melt after relocation; the corresponding melt mass in the sumps for the conventional fuel and ATF scenarios are shown in Table 4. In both cases, the initial melt temperature was taken equal to 2750 K. In terms of simulating decay heat within the core debris, the decay heat function developed by Robb et al. [8] was used in this study.

Regarding other containment conditions, these were also modeled using the same assumptions made by Robb et al. [8]; i.e., the concrete type was taken as siliceous, and the containment pressure was set equal to 0.75 MPa. The balance of the user-controlled phenomenological modeling assumptions that can be specified as part of the code input were set equal to the best-estimate settings developed as part of the code validation process [7].

4. RESULTS

As noted above, only scenarios based on MAAP melt pour conditions are specifically addressed herein. In order to form a basis for evaluating the potential impact of ATF on ex-vessel core melt behavior, cases were run with conventional clad fuel as well as ATF so that the results could be directly compared. Two scenarios were considered; the first is one in which the cavity remains dry, representing the worst case in terms of the extent of cavity ablation and combustible gas production. The second scenario examines the situation in which water is introduced over the core debris immediately after melt relocation to look at the impact of ATF on debris coolability. All calculations were initiated at 607 minutes, which is the time at which the RPV lower head fails in the MAAP analysis after the reactor was scrammed. The dry cavity calculations were carried out for 24 hours after vessel failure. The wet cavity cases were carried out until the debris was quenched and stabilized, thereby terminating concrete ablation and combustible gas production by metals oxidation in the melt.

The predicted cavity ablation, melt temperature, noncondensable-combustible gas production, integrated chemical reaction heat, and melt-atmosphere heat flux are shown in Figures 2-6, respectively, for the *dry cavity* cases. As is evident from these figures, for this

scenario the ATF has a beneficial impact on the accident sequence in that it reduces the overall cavity ablation and combustible gas production from core-concrete interaction over the course of a 24 hour transient. This is predominately due to the fact that a portion of the Si is assumed to be sequestered as chemically inert SiC in the oxide phase in this work; see Table 4. The validity of this assumption remains to be determined. However, note that the melt temperature steadily declines over the course of the calculation (Figure 3), which would increase the thermodynamic stability of this material when in solution with UO_2 [6].

The analogous predictions of cavity ablation, melt temperature, noncondensable-combustible gas production from core-concrete interaction, melt-water heat flux, and integrated chemical reaction heat are provided in Figures 7-11, respectively, for the *wet cavity* cases. As noted earlier, in these graphs the data extends out to the point where the core debris was quenched and thermally stabilized in each calculation. As is evident from these figures, for this scenario the ATF still has a beneficial impact on the accident sequence since there is small overall decrease in cavity ablation and combustible gas production by the time the core debris is stabilized. However, the reduction in concrete ablation is not as significant as for the dry cavity case, and this is due to the fact that SiO_2 produced as a byproduct of Si reactions with concrete decomposition gases (Table 1) has a very low thermal expansion coefficient (Table 3). In terms of phenomenological mechanisms modeled in CORQUENCH that can quench and stabilize core debris, there are two: i) *melt eruptions* (driven by concrete decomposition gases leading to melt entrainment into overlying water that forms a coolable debris bed over the crust), and ii) *water ingression* (into cracks and fissures within the crust that develop during cooldown of the core

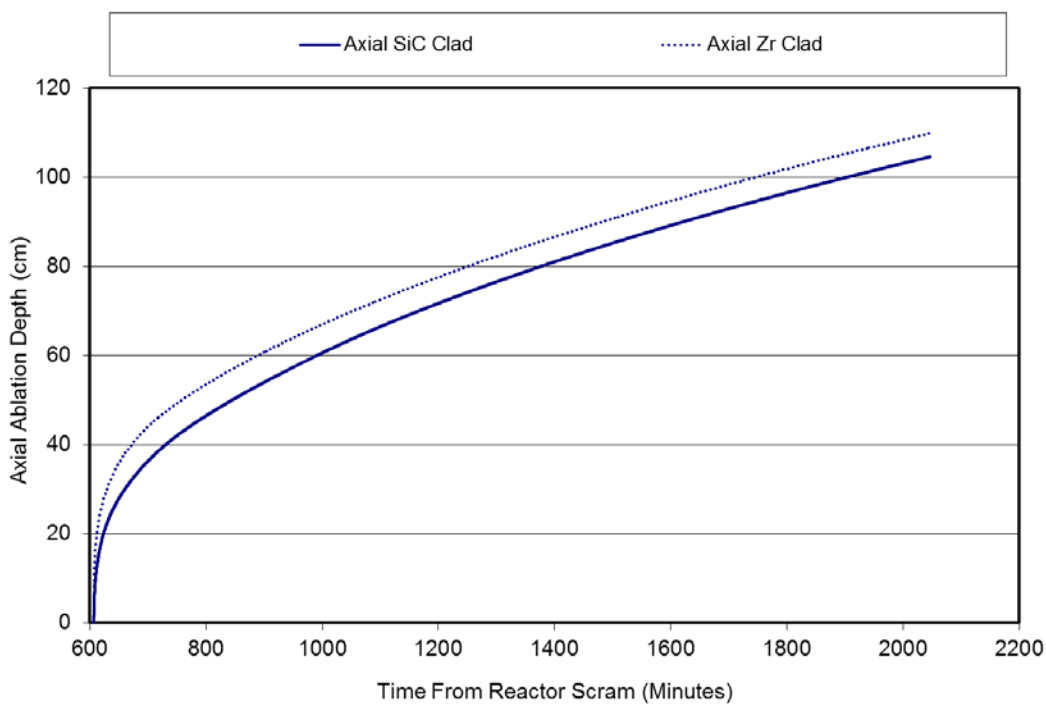

Figure 2. Sump Ablation Depth vs. Time for a MAAP Dry Cavity Scenario for Zr- and SiC-Clad UO_2 Fuel Systems.

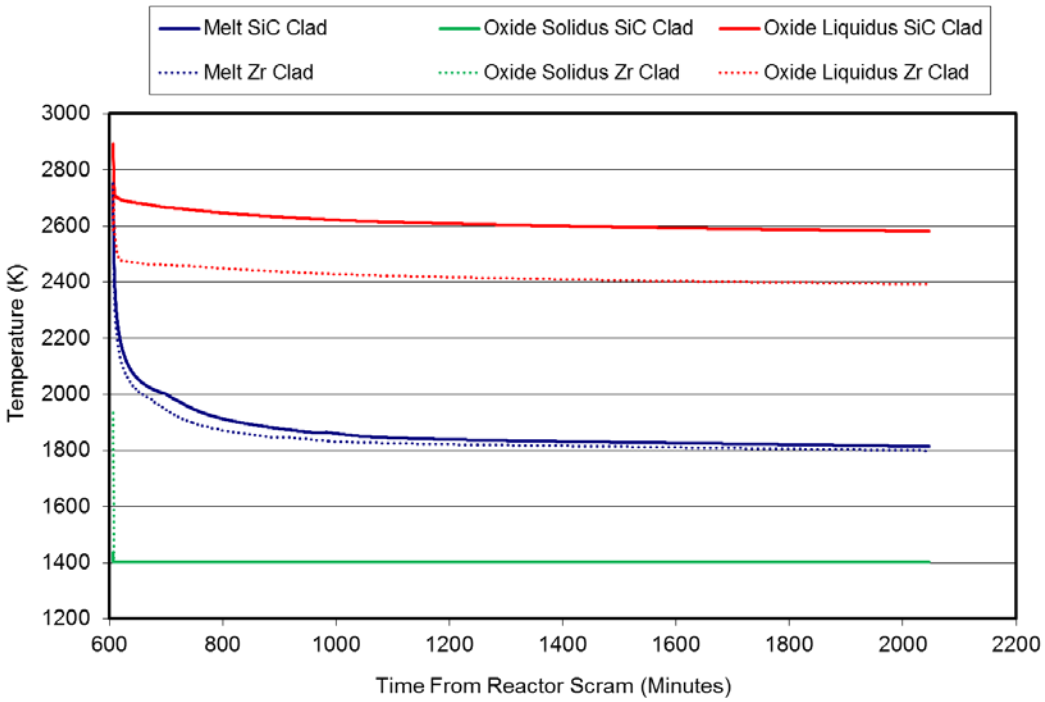

Figure 3. Melt Temperatures vs. Time for a MAAP Dry Cavity Scenario for Zr- and SiC-Clad UO_2 Fuel Systems.

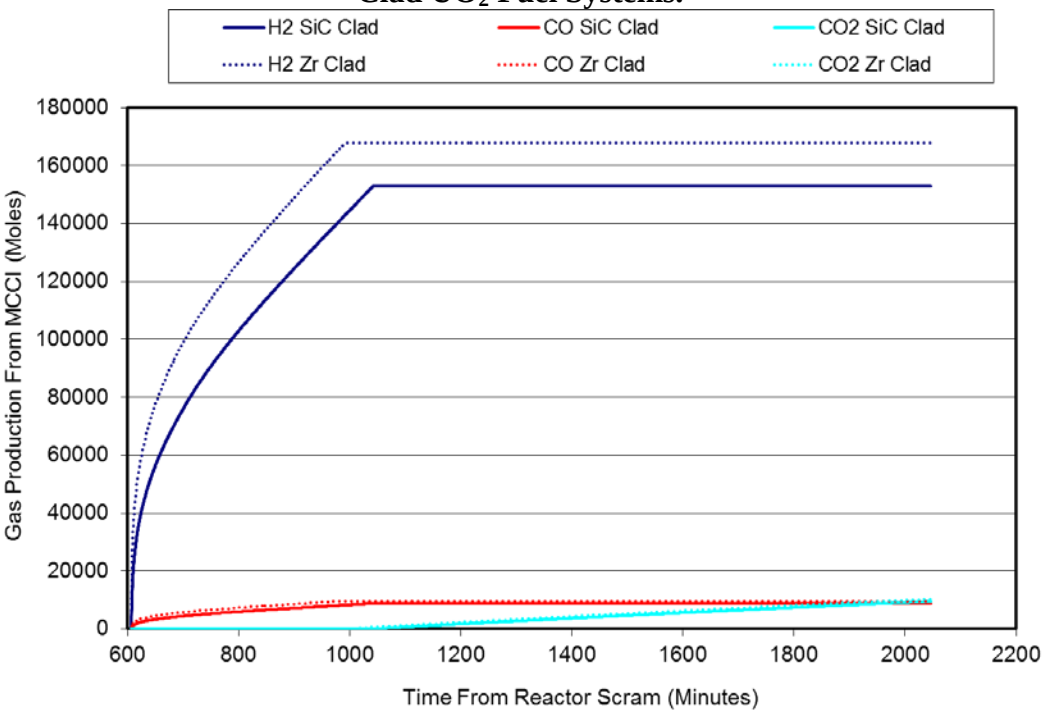

Figure 4. Combustible Gas Production from MCCI vs. Time for a MAAP Dry Cavity Scenario for Zr- and SiC-Clad UO_2 Fuel Systems.

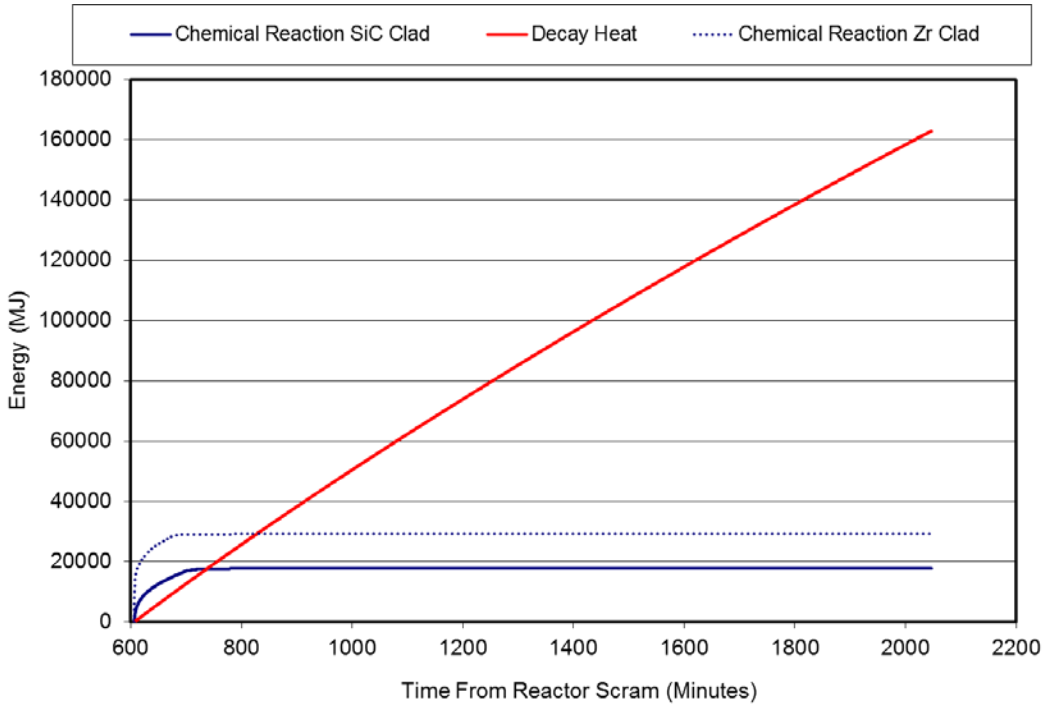

Figure 5. Integrated Decay Heat and Chemical Reaction Heat from MCCI vs. Time for a MAAP Dry Cavity Scenario for Zr- and SiC-Clad UO_2 Fuel Systems.

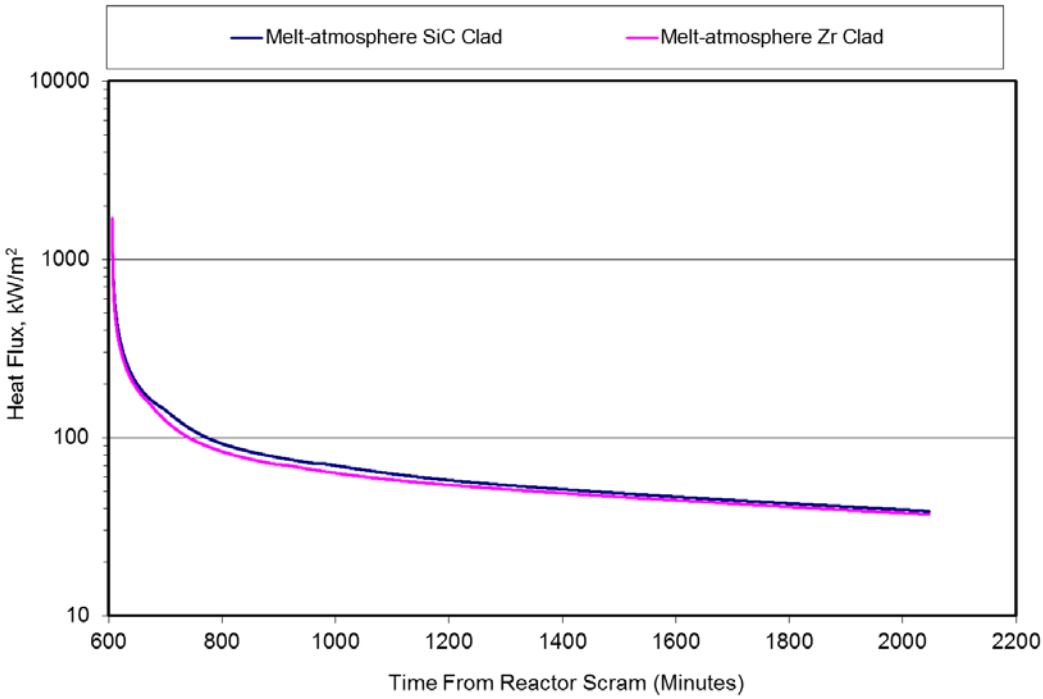

Figure 6. Melt-Atmosphere Heat Flux vs. Time for a MAAP Dry Cavity Scenario for Zr- and SiC-Clad UO_2 Fuel Systems.

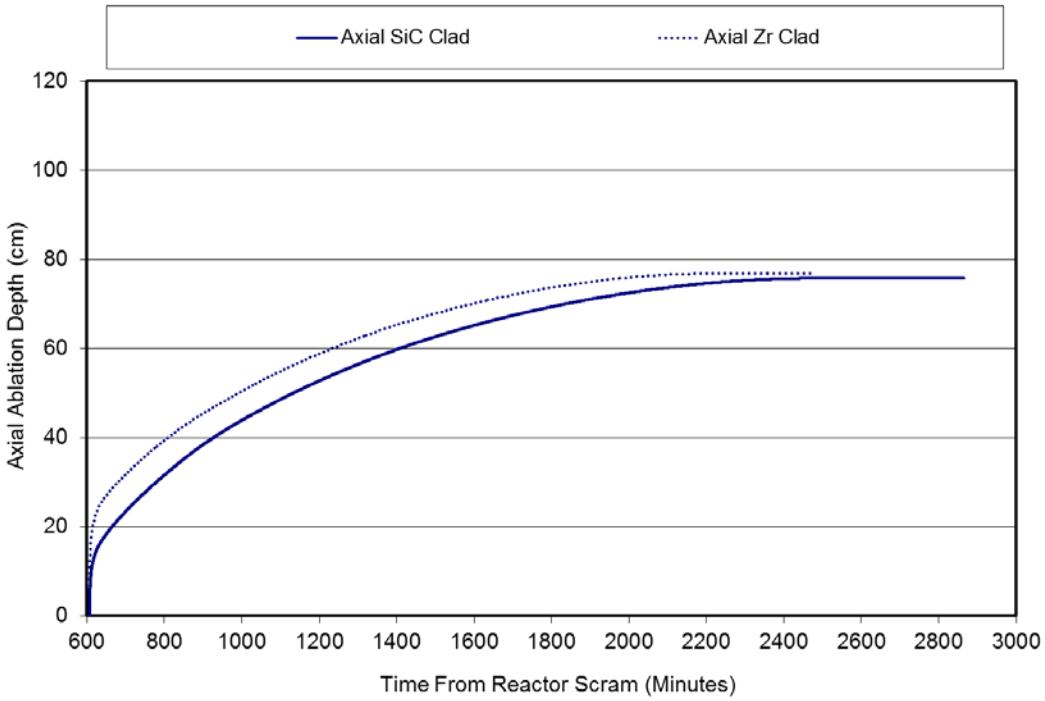

Figure 7. Sump Ablation Depth vs. Time for a MAAP Wet Cavity Scenario for Zr- and SiC-Clad UO_2 Fuel Systems.

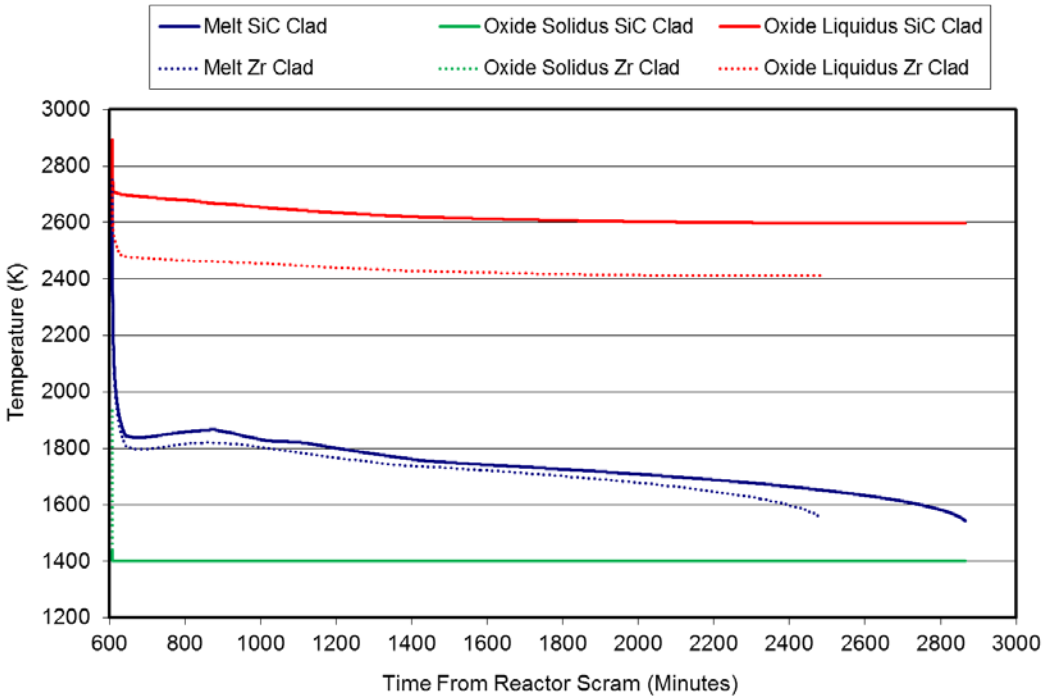

Figure 8. Melt Temperatures vs. Time for a MAAP Wet Cavity Scenario for Zr- and SiC-Clad UO_2 Fuel Systems.

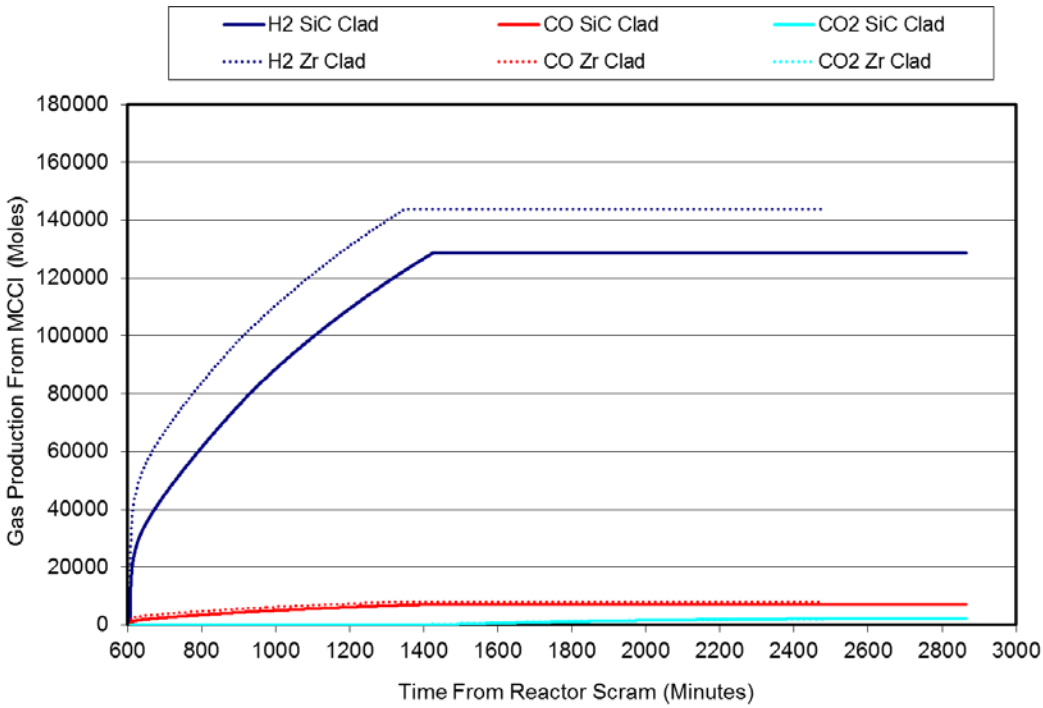

Figure 9. Combustible Gas Production from MCCI vs. Time for a MAAP Wet Cavity Scenario for Zr- and SiC-Clad UO_2 Fuel Systems.

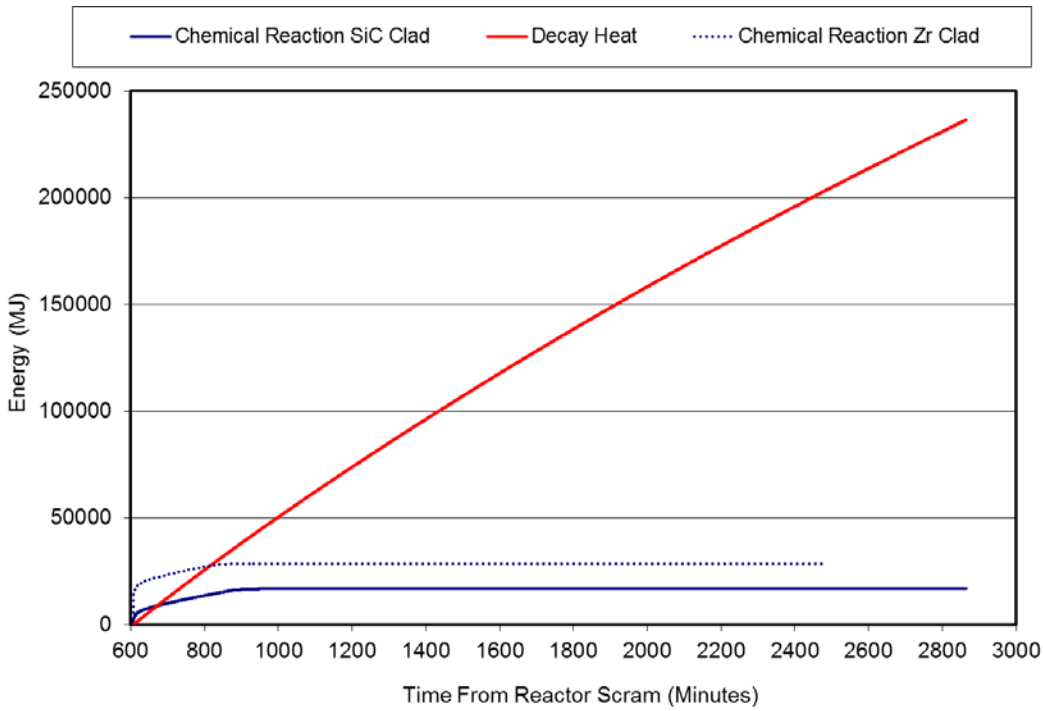

Figure 10. Integrated Decay Heat and Chemical Reaction Heat from MCCI vs. Time for a MAAP Wet Cavity Scenario for Zr- and SiC-Clad UO_2 Fuel Systems.

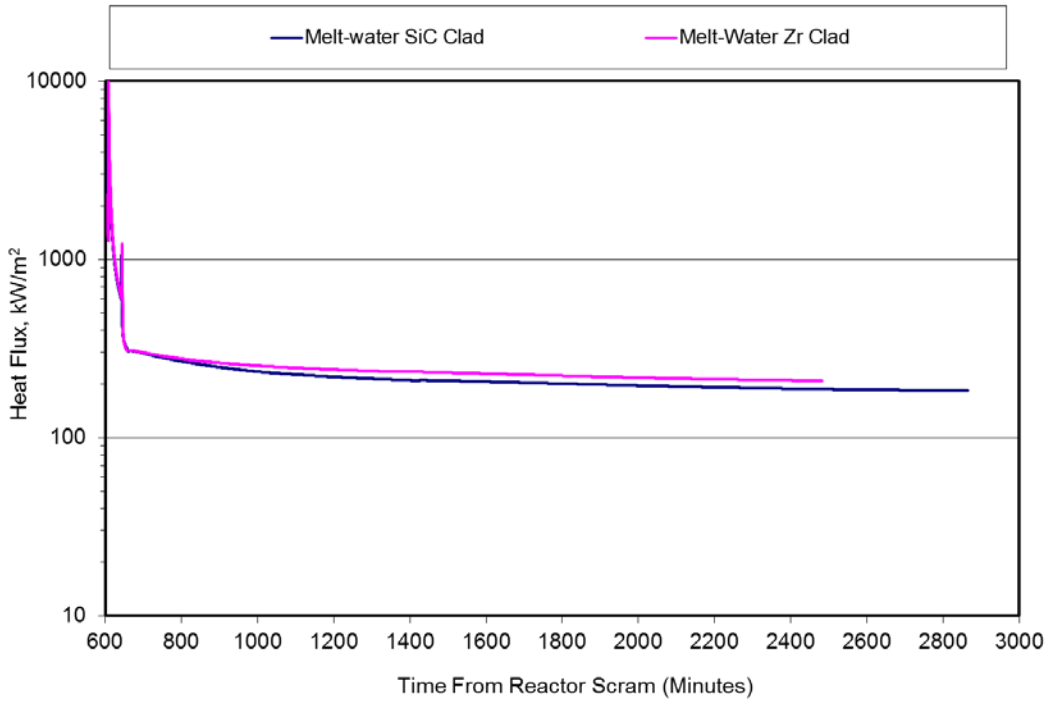

Figure 11. Melt-Water Heat Flux vs. Time for a MAAP Wet Cavity Scenario for Zr- and SiC-Clad UO_2 Fuel Systems.

debris). The predominant debris cooling mechanism for scenarios involving this concrete type is water ingression, and this is due to the relatively low gas content of siliceous concrete. The reduction in the thermal contraction coefficient in the crust due to the increased ingress of SiO_2 as Si is oxidized slightly reduces the effectiveness of the water ingression for the ATF case. This effect is best illustrated in Figure 11 that shows the slightly reduced debris cooling rate for the ATF case relative to the Zr-clad case.

5. SUMMARY AND CONCLUSIONS

An initial effort has been made to upgrade the CORQUENCH code in order to be able to analyze ex-vessel core-concrete interaction and debris coolability for late phase core melt compositions that may develop with accident tolerant fuels. The specific ATF type considered in this study was SiC-clad UO_2. In terms of upgrades that were made to treat this scenario, the code was restructured to include Si and SiC as melt constituents. The metals oxidation hierarchy was also restructured to include Si. The reaction rate of the Si metal was assumed to be controlled by the rate of concrete decomposition gas production during core-concrete interaction. Earlier thermodynamic equilibrium calculations [6] indicate that for a given temperature and pressure, some amount SiC would remain in the core debris in equilibrium with the other chemical species. In this initial study, any SiC present in the debris relocated from the reactor vessel was assumed

to reside as an inert material within the oxide phase (consisting of UO_2, concrete, structural steel metals, and their corresponding oxides). Revisions to the property subroutines were also made to account for the presence of Si and SiC in the corium enthalpy-temperature, thermal conductivity, density, melt solid fraction, solidus-liquidus temperature, emissivity, viscosity, and crust mechanical strength evaluations.

A MAAP SBO sequence involving breach of the RPV and follow-on MCCI was considered as part of this study. In order to form a basis for evaluating the potential impact of ATF on ex-vessel core melt behavior, cases were run with conventional clad fuel as well as ATF so that the results could be directly compared. Two scenarios were considered; the first is one in which the cavity remains dry, representing the worst case in terms of the extent of cavity ablation and combustible gas production. The second scenario examines the situation in which water is introduced over the core debris immediately after melt relocation to look at the impact of ATF on debris coolability.

The results for the dry cavity case indicate that ATF has a beneficial impact on the accident sequence in that it reduces the overall cavity ablation and combustible gas production over the course of the 24 hour transient. The same conclusion applies to the wet cavity case, but the benefit is not as large due to the fact that SiO_2 produced as a byproduct of Si reactions with concrete decomposition gases has a very low thermal expansion coefficient which acts to degrade the water ingression cooling mechanism that contributes to overall debris coolability.

6. REFERENCES

1. B. A. Pint, K. A. Terrani, M. P. Brady, T. Cheng, J. R. Keiser, "High Temperature Oxidation of Fuel Cladding Candidate Materials in Steam-Hydrogen Environments," *J. Nucl. Mater.* 440 (2013) 420-427.
2. T. Cheng, J. R. Keiser, M. P. Brady, K. A. Terrani, B. A. Pint, "Oxidation of Fuel Cladding Materials in Steam Environments at High Temperature and Pressure," *J. Nucl. Mater.* 427 (2012) 396-400.
3. L. J. Ott, K. R. Robb, D. Wang, "Preliminary Assessment of ATFs on LWR during Normal Operation and under DB and BDB Accident Conditions," *J. Nucl. Mater.* (2013), http://dx.doi.org/10.1016/j.jnucmat.2013.09.052.
4. K. R. Robb, "Analysis of the FeCrAl Accident Tolerant Fuel Concept Benefits During BWR Station Blackout Accidents," NURETH-16, Chicago, IL, August 30-September 4, 2015.
5. B.J. Merrill and S. M. Bragg-Sitton, "SiC Modifications to MELCOR for Severe Accident Analysis Applications," in proceedings of the *LWR Fuel Performance Meeting, Top Fuel 2013*, Charlotte, NC, September 15-19, 2013.

6. M. T. Farmer, L. Leibowitz, K. A. Terrani, and K. R. Robb, “Scoping Assessments of ATF Impact on Late-Stage Accident Progression Including Molten Core–Concrete Interaction,” *J. Nucl. Mater*. (2014), 10.1016/j.jnucmat.2013.12.022.
7. M. T. Farmer, “The CORQUENCH Code for Modeling of Ex-Vessel Corium Coolability under Top Flooding Conditions, Code Manual – Version3.03,” OECD/MCCI-2010-TR03, March 2010.
8. K. R. Robb, M. W. Francis, M. T. Farmer, “Enhanced Ex-Vessel Analysis for Fukushima Daiichi Unit 1: Melt Spreading and Core-Concrete Interaction Analyses with MELTSPREAD and CORQUENCH,” ORNL/TM-2012/455, February 2013.
9. H. Ellingham, "Reducibility of oxides and sulfides in metallurgical processes," *J. Soc. Chem. Ind.* 63 (1944) 125-133.
10. H. Thompson, M. T. Farmer, J. K. Fink, D. R. Armstrong, and B. W. Spencer, “ACE Phase C Final Report: Volume I-MCCI Thermal hydraulic Results,” EPRI/ACE-TR-C42, September, 1997.
11. R. G. Munro, “Material Properties of a Sintered alpha-SiC,” *J. Physical and Chemical Reference Data* (1997) 26 1195-1203.
12. P. D. Desai, “Thermodynamic Properties of Iron and Silicon,” *J. Phys. Chem. Ref. Data*, Vol. 15, No. 3, 1986.
13. V. A. Kirillin, A. E. Sheindlin, and V. Ya. Chekhovskoi, “Enthalpy and Specific Heat of Silicon Carbide at High Temperatures,” Refractory Carbides, Consultants Bureau, New York, 1974.
14. L. V. Gurvich and I. Veyts, editors, “Thermodynamic Properties of Individual Substances: Elements and Compounds,” p. 299, CRC Press, September 1, 1990.
15. C. Y. Ho, R. W. Powell, and P. E. Liley, “Thermal Conductivity of the Elements: A Comprehensive Review,” *J. of Physical and Chemical Reference Data*, Vol. 3 (1974).
16. W. N. Sharpe et al., “Measurements of Young’s Modulus, Poisson’s Ratio, and Tensile Strength of Polysilicon,” *Proceedings of the Tenth IEEE International Workshop on Microelectromechanical Systems*, Nagoya, Japan, 424-429 (1997).
17. R. Hull, Ed., “Properties of Crystalline Silicon,” The Institute of Electrical Engineers, London, England, 1999.
18. K. Petersen, “Silicon as a Mechanical Material,” Proceedings of the IEEE, Vol. 70, No. 5, p. 420-456 (1982).
19. R. Gauntt et al., “Fukushima Daiichi Accident Study (Status as of April 2012),” SAND2012-6173, Sandia National Laboratories, 2012.
20. D. Luxat et al., “Fukushima Technical Evaluation: Phase 1 - MAAP5 Analysis,” EPRI Technical Report 1025750 (April 2013).
21. D. Luxat, D. Kalinich, and J. Hanophy, EPRI-3002004449, “Modular Accident Analysis Program (MAAP) – MELCOR Crosswalk, Phase 1 Study,” EPRI, Palo Alto, CA, 2014
22. P. Hofmann, “Current Knowledge on Core Degradation Phenomena, a Review,” *J. Nucl. Mater*. 270 (1999) 194-211.

Nuclear Engineering Division
Argonne National Laboratory
9700 South Cass Avenue, Bldg.208
Argonne, IL 60439

www.anl.gov

Argonne National Laboratory is a U.S. Department of Energy
laboratory managed by UChicago Argonne, LLC